Published in final edited form as:

Sci Transl Med. 2019 July 03; 11(499): . doi:10.1126/scitranslmed.aav4634.

CFTR-PTEN–dependent mitochondrial metabolic dysfunction promotes *Pseudomonas aeruginosa* airway infection

Sebastián A. Riquelme[1,*], **Carmen Lozano**[2,*], **Ahmed M. Moustafa**[3,*], **Kalle Liimatta**[1], **Kira L. Tomlinson**[1], **Clemente Britto**[4], **Sara Khanal**[4], **Simren K. Gill**[1], **Apurva Narechania**[5], **Jose M. Azcona-Gutiérrez**[6], **Emily DiMango**[7], **Yolanda Saénz**[2], **Paul Planet**[3], **Alice Prince**[1,†]

[1]Department of Pediatrics, Columbia University, New York, NY 10032, USA.

[2]Area de Microbiología Molecular, Centro de Investigación Biomédica de la Rioja (CIBIR), Microbiología Molecular, Logroño, LG 26006, Spain.

[3]Department of Pediatrics, Perelman School of Medicine, University of Pennsylvania and Children's Hospital of Philadelphia, Philadelphia, PA 19104, USA.

[4]Section of Pulmonary, Critical Care, and Sleep Medicine, Yale University School of Medicine, New Haven, Connecticut, CT 06520, USA.

[†]Corresponding author. asp7@columbia.edu.

[*]These authors contributed equally to this work.

Author contributions: S.A.R. proposed the central hypothesis, conducted the experiments, and wrote the manuscript. C.L., A.M.M., and P.P. conducted the experiments and wrote the manuscript. C.B., S.K., K.L., K.L.T., and S.K.G. conducted the experiments. A.N. conducted the sequencing and genomic analyses. Y.S. and J.M.A.-G. provided CF isolates. E.D. provided CF PBMCs. A.P. proposed the central hypothesis and wrote the manuscript.

SUPPLEMENTARY MATERIALS

stm.sciencemag.org/cgi/content/full/11/499/eaav4634/DC1

Materials and Methods

Fig. S1. PTEN affects mitochondrial membrane potential and assimilation of metabolites.

Fig. S2. HIF1α is not increased in PTEN-null cells.

Fig. S3. PTEN regulates succinate secretion during infection with *P. aeruginosa*.

Fig. S4. PTEN is reduced in patients with *CFTR* mutations.

Fig. S5. Succinate in BAL is increased in *P. aeruginosa*–infected $CFTR^{\Delta F508/\Delta F508}$ mice.

Fig. S6. High succinate induces oxidative stress and metabolic adaptation in *P. aeruginosa* in LB and CF sputum–like media.

Fig. S7. Succinate-stressed WT *P. aeruginosa* produce larger colonies in succinate-free LB agar plates.

Fig. S8. Succinate-stressed *P. aeruginosa* biofilms are more tolerant to succinate.

Fig. S9. The PTEN-succinate axis does not regulate *S. aureus* adaptation to the airway.

Fig. S10. Phenotypic characterization of *P. aeruginosa* strains recovered over 4 years from the CF airway.

Fig. S11. Mucoid and SCV CF isolates have differential preference for succinate, acetate, and L-threonine compared with PAO1.

Fig. S12. CF-adapted *P. aeruginosa* excrete succinate.

Fig. S13. Host-adapted *P. aeruginosa* induce less secretion of proinflammatory cytokines in the airway.

Fig. S14. IL-1β induced by metabolically adapted *P. aeruginosa* isolates is not trapped inside neutrophils.

Fig. S15. IRG1 expression by resident alveolar macrophages and neutrophils in *P. aeruginosa*–infected mice.

Fig. S16. Clinical isolates of *P. aeruginosa* do not induce cell death in $IRG1^{+}$ BAL monocytes.

Table S1. *CFTR* genotype and *P. aeruginosa* airway abundance in healthy patients and patients with CF.

Table S2. Pathoadaptive mutations conserved in all 17 CF *P. aeruginosa*.

Table S3. Accession numbers for *P. aeruginosa* isolates.

Table S4. PAMPs found mutated in all CF *P. aeruginosa* isolates.

Table S5. Sequences of the primers used for qRT-PCR.

Data file S1. Raw data from figures.

Competing interests: The authors declare that they have no competing interests.

Data and materials availability: All data associated with this study are present in the paper or the Supplementary Materials. *P. aeruginosa* genome isolates are available at GenBank; genome accession numbers are given in table S3. Raw data from figures are in data file S1.

[5]American Museum of Natural History, New York, NY 10024, USA.

[6]Departamento de Diagnóstico Biomédico. Laboratorio de Microbiología, Hospital San Pedro, Logroño, LG 26006, Spain.

[7]Department of Medicine, Columbia University, New York, NY 10032, USA.

Abstract

Phosphatase and tensin homolog deleted on chromosome 10 (PTEN) is a tumor suppressor best known for regulating cell proliferation and metabolism. PTEN forms a complex with the cystic fibrosis (CF) transmembrane conductance regulator (CFTR) at the plasma membrane, and this complex is known to be functionally impaired in CF. Here, we demonstrated that the combined effect of PTEN and CFTR dysfunction stimulates mitochondrial activity, resulting in excessive release of succinate and reactive oxygen species. This environment promoted the colonization of the airway by *Pseudomonas aeruginosa*, bacteria that preferentially metabolize succinate, and stimulated an anti-inflammatory host response dominated by immune-responsive gene 1 (IRG1) and itaconate. The recruitment of myeloid cells induced by these strains was inefficient in clearing the infection and increased numbers of phagocytes accumulated under CFTR-PTEN axis dysfunction. This central metabolic defect in mitochondrial function due to impaired PTEN activity contributes to *P. aeruginosa* infection in CF.

INTRODUCTION

The pulmonary pathology associated with cystic fibrosis (CF) consists of dysregulated airway inflammation and excess reactive oxygen species (ROS) that fail to eradicate infection, typically due to *Pseudomonas aeruginosa*, in over 70% of patients (1, 2). In addition to its function as a chloride channel, membrane-attached CF transmembrane conductance regulator (CFTR) normally acts as a scaffold for several proteins, including the phosphatase and tensin homolog deleted on chromosome 10 (PTEN), resulting in substantially diminished PTEN activity in cells harboring *CFTR* mutations (3). PTEN is a central regulator of cell metabolic activity. It is involved in glycolysis and lipid and mitochondrial oxidative metabolism and also controls the activity of phosphatidylinositol 3-kinase (PI3K) by regulating Akt and numerous downstream effectors (4–6). In response to increased metabolic requirements, such as during infection, cells use aerobic glycolysis to generate energy (4, 7). Increased glycolysis fills the energetic gap left by mitochondria, whose function is repurposed to produce ROS (anion superoxide: $O_2{}^{*-}$) as well as pro- and anti-inflammatory metabolites during infection. Whether PTEN deregulation in CF affects the mitochondrial reaction to infection remains poorly characterized.

The metabolic response of phagocytes and epithelial cells to bacterial infection can have major immunological consequences. Cytosolic succinate promotes the stabilization of hypoxia-induced factor 1α (HIF1α), a transcription factor (fig. S1A) (8) that, along with mitochondrial ROS, induces the generation of the potent proinflammatory cytokine interleukin-1β (IL-1β) (9, 10). IL-1β and ROS responses are important in fighting infection but must be regulated to avoid excessive tissue damage. Inflammatory signaling is limited, in part, by the immune-responsive gene 1 (*IRG1*). In response to lipopolysaccharide (LPS),

IRG1 converts cis-aconitate into itaconate (fig. S1A), a metabolite with central anti-inflammatory functions (11). Itaconate inhibits the activity of succinate dehydrogenase (SDH; which is complex II in mitochondrial respiration and a major source of mitochondrial ROS), limiting its toxic effects and IL-1β production (12, 13). Decreased SDH activity results in the accumulation and release of succinate from mitochondria, and this metabolite is able to reach the extracellular milieu (12, 14). Such excreted succinate would be expected to favor the colonization of the airway by microbes that preferentially metabolize the compound. PTEN-deficient epithelial cells and patients with *PTEN* mutations have been noted to have increased mitochondrial ROS and increased extracellular succinate, respectively, suggesting that this phosphatase might also regulate the accumulation of ROS and succinate in CF cells (6, 15, 16).

We postulated that the lack of PTEN function in CF mitochondria would affect the normal succinate/itaconate balance that regulates the response to infection. Without the appropriate regulatory function of PTEN, we expected that ROS would accumulate in cells, increasing compensatory anti-inflammatory IRG1 activity, in turn inhibiting SDH activity and resulting in excessive succinate release. We hypothesized that *P. aeruginosa*, bacteria that preferentially consume succinate as directed by their catabolite repressor locus (*crc*) (17–21), would then consume the abundant succinate in the CF airway, facilitating lung colonization and persistent infection. In this study, we demonstrate how PTEN contributes to mitochondrial metabolism by affecting both IRG1 and succinate production, with important consequences on airway inflammation and the selection of *P. aeruginosa* adapted for chronic infection.

RESULTS

PTEN deficiency triggers pro-oxidant mitochondrial metabolism

We used human epithelial cell lines lacking PTEN to establish the importance of PTEN in the mitochondrial metabolic pathways that regulate host immunity (fig. S1A). Compared with PTEN-sufficient cells, there was a slight but significant increase ($P < 0.01$) in the mitochondrial membrane potential ($\Delta\Psi$) (fig. S1B) and a significant generation of oxidants ($P < 0.0001$) in the PTEN-null cells (Fig. 1, A and B). This confirmed previous findings with other PTEN-null cell lines (15) and suggested a dysfunction in mitochondrial metabolism. We observed altered metabolism of tricarboxylic acid (TCA) cycle intermediates, with significantly ($P < 0.05$) increased mitochondrial assimilation of isocitrate (Fig. 1C) and increased isocitrate dehydrogenase (IDH) protein ($P < 0.0001$) (Fig. 1D), both of which have immunoregulatory activity (22, 23). IDH-mediated isocitrate catabolism produces NADH (reduced form of nicotinamide adenine dinucleotide), which stimulates mitochondrial complex I and ROS production (fig. S1A) (24, 25). We also observed increased cellular assimilation of glyceraldehyde-3-phosphate (G3P) (fig. S1C), another potential pro-ROS complex I and II stimulator (26) in the absence of PTEN. These findings suggested that a lack of PTEN induces increased mitochondrial and cellular assimilation of metabolites that predominantly feed ROS production through complex I.

Lack of PTEN drives antioxidant IRG1 function and succinate accumulation

We hypothesized that the excessive ROS production observed in PTEN-deficient mitochondria could force the cell to trigger an antioxidant response. Although PTEN did not control mitochondrial succinate uptake (Fig. 1C) or cellular SDH amounts (complex II) (Fig. 1E), we observed that total SDH activity was significantly decreased in *PTEN*$^{-/-}$ cells compared with wild-type (WT) controls ($P < 0.0001$) (Fig. 1F), consistent with inhibition of mitochondrial complex II to balance ROS production (12, 27). We also noted significantly increased expression of the SDH inhibitor and antioxidant IRG1 in *PTEN*$^{-/-}$ cells ($P < 0.0001$) (Fig. 1G) (12). SDH inactivation by IRG1 was accompanied by increased excretion of succinate (Fig. 1H). We confirmed that released succinate was not derived from glutamine/GABA (γ-aminobutyric acid) metabolism (fig. S1A), as assimilation of both intermediates was unchanged in the absence of PTEN (Fig. 1C) and HIF1α was not increased (fig. S2) (9).

Succinate secretion due to lack of PTEN is compounded by *P. aeruginosa* infection

Succinate excretion and IRG1 activity are normally increased in response to infection (12). We next examined how PTEN would contribute to succinate secretion in response to the major CF pathogen *P. aeruginosa*. In WT epithelial cells and alveolar macrophages exposed to *P. aeruginosa*, we observed that depletion of PTEN was accompanied by increased release of succinate, both in vivo (fig. S3) and in vitro (Fig. 1, H and I). Pulmonary infection in mice lacking PTEN-long, the translational variant of PTEN that is specifically involved in mitochondrial regulation (3, 28, 29), was associated with 10-fold greater succinate accumulation into the airways than WT controls, reaching concentrations up to 500 mM (Fig. 1J). Thus, in the setting of *P. aeruginosa* infection, PTEN deficiency is associated with even greater succinate release than in normal cells.

PTEN deficiency drives ROS and IRG1-SDH deregulation in CF mitochondria

Having found that PTEN function is important in regulating mitochondrial ROS and the succinate/itaconate balance, we examined whether PTEN dysfunction contributes to the increased ROS production that characterizes the inflammatory component of CF airway disease (1, 30). Using confocal imaging, we demonstrated in human epithelial cells that the majority of CFTR pixels within mitochondrial boundaries colocalized with the mitochondrial outer membrane protein TOMM20 (Fig. 2, A to D). The majority of CFTR (77%) was outer membrane associated, and of that fraction, 69% colocalized with PTEN, consistent with the formation of a functional complex.

We replenished PTEN, reduced in CF cells (fig. S4), in ΔF508/ΔF508 *CFTR* human epithelial cell lines to establish its role in mitochondrial function. Transfection of CF cells with a *PTEN-GFP*–encoding adenovirus [green fluorescent protein–positive (GFP^+) cells] resulted in a significantly reduced population of $O_2{}^{*-}$-producing cells ($P < 0.0001$) compared with cells infected with a GFP-encoding adenovirus control (Fig. 2, E and F). Likewise, lentiviral delivery of WT *CFTR* to ΔF508/ΔF508 *CFTR* cells also increased PTEN expression (Fig. 2G) and reduced production of mitochondrial ROS compared with cells treated with an empty vector (Fig. 2H). Restoration of CFTR-PTEN in CF cells reduced mitochondrial consumption of isocitrate (Fig. 2I) and was accompanied by a slight

increase in IDH (Fig. 2J). Small changes in SDH (Fig. 2K), but significantly increased SDH activity ($P < 0.0001$) (Fig. 2L), were associated with significantly reduced expression of IRG1 ($P < 0.001$) (Fig. 2M). This finding suggested that CFTR influences SDH function through the PTEN-IRG1 axis, which is central to ROS generation and immunoregulation (11–13, 31).

P. aeruginosa increases excessive succinate secretion by CF cells

We predicted that lack of a CFTR-PTEN interaction would favor succinate secretion from CF cells. We confirmed that lack of PTEN in patients with CF impaired mitochondrial activity, promoting a 10-fold increase in succinate accumulation in airway fluid compared with healthy controls (Fig. 2N and table S1). Likewise, CF peripheral blood mononuclear cells (PBMCs) secreted significantly more succinate than normal control cells both before ($P < 0.001$) and after *P. aeruginosa* infection ($P < 0.01$) (Fig. 2O), which was consistent with their reduced expression of intracellular PTEN (fig. S4). In a *Cftr*$^{\Delta F508/\Delta F508}$ gut-corrected mouse model, broncheoalveolar lavage (BAL) from 60% of PAO1-infected mice (three of five) had succinate concentrations above those observed in control airways (fig. S5). Thus, the excess release of succinate from CF cells can be attributed to lack of PTEN and is further compounded by *P. aeruginosa* infection.

High succinate induces oxidative stress in *P. aeruginosa*

We tested the effects of succinate (from 7 to 500 mM) on the growth rate, biofilm formation, and metabolic activity of a laboratory strain of *P. aeruginosa* (PAO1) in vitro. PAO1 growth in Luria Bertani (LB) was maintained in succinate and only partially inhibited at 500 mM succinate (Fig. 3A and fig. S6A), a concentration observed in *Ptenl*$^{-/-}$ mice broncheoalveolar fluid (Fig. 1J). However, succinate reduced biofilm production at all concentrations tested (Fig. 3A), suggesting that *crc*-directed succinate assimilation repressed pathways that *P. aeruginosa* use to generate biofilm (fig. S6B) (20, 32). In CF artificial sputum media (33), *P. aeruginosa* growth and biofilm formation were enhanced by increasing concentrations of succinate until returning to initial values at 500 mM succinate (fig. S6C). These data suggested that the CF airway composition would promote the metabolic effects that succinate has on *P. aeruginosa*. Immediately after a 2-hour exposure to high succinate (500 mM), *P. aeruginosa* accumulated significantly more $O_2{}^{*-}$ ($P < 0.0001$) compared with bacteria exposed to 10-fold less (50 mM) or to no succinate (Fig. 3B and fig. S6D). These findings indicate that excess succinate causes metabolic stress in *P. aeruginosa* and induces biofilm production and growth.

Succinate-stressed *P. aeruginosa* display metabolic reprogramming

To control the oxidative stress caused by succinate, we predicted that *P. aeruginosa* would use alternative metabolic routes to reduce ROS, such as the antioxidant glyoxylate shunt and the Entner-Doudoroff pathway (32, 34, 35). We found that *P. aeruginosa* grown in high (500 mM) succinate overnight showed increased assimilation of acetate and L-threonine (Fig. 3C), two carbon sources that feed the glyoxylate shunt that bypasses the $O_2{}^{*-}$-generating SDH and IDH activity of the TCA cycle (fig. S6B) (32, 35, 36). Growth on high succinate also increased assimilation of the α-D-glucose dimer D-trehalose consistent with Entner-Doudoroff activity to generate antioxidant extracellular polysaccharides such as alginate

(Fig. 3C and fig. S6B) (37–39). Only 50 mM succinate in CF sputum–like media was required to augment the consumption of α-D-glucose and D-mannose by PAO1 cells, changes that persisted at higher succinate concentrations (fig. S6E). In this CF media, high succinate induced more consumption of pro-glyoxylate shunt L-threonine and pro–Entner-Doudoroff D-trehalose by *P. aeruginosa* (fig. S6E). No major changes due to high succinate were observed with assimilation of TCA cycle intermediates in CF sputum–like media (fig. S6E).

We observed that the PAO1 clones selected in high succinate conditions had increased colony size on agar plates (fig. S7), suggesting a gain in extracellular polysaccharide production. *AlgD*, the gene that produces alginate (fig. S6B), was significantly overexpressed ($P < 0.001$) in succinate-stressed PAO1 compared with control PAO1 (Fig. 3D), consistent with the development of a mucoid-like phenotype, pathognomonic for mucoid *P. aeruginosa* infection in CF. *Glk*, a gene that regulates the Entner-Doudoroff pathway and provides *algD* with α-D-glucose derivatives, was also up-regulated (Fig. 3D). Glyoxylate shunt genes *aceA* and *glcB*, which bypass the succinate-mediated ROS production and feed Entner-Doudoroff activity (fig. S6B), were similarly increased in succinate-stressed cells (Fig. 3D). Expression of the bacterial SDH genes *sdhA-B* was decreased in the succinate-adapted clones (Fig. 3D and fig. S6B), likely to avoid oxidants generated by succinate catabolism. *Crc* expression (Fig. 3D) and obligatory succinate assimilation (Fig. 3C) were not changed by exposure to high succinate. PAO1 on high succinate continued producing biofilm under these conditions (fig. S8), a process not necessarily requiring alginate production (40). Thus, in vitro exposure to high succinate induces metabolic adaptation in *P. aeruginosa* by up-regulating the antioxidant glyoxylate shunt and Entner-Doudoroff extracellular polysaccharide pathways.

Succinate-driven metabolic adaptation increases airway colonization by *P. aeruginosa*

We next evaluated how metabolic adaptation to succinate by *P. aeruginosa* affected airway colonization. We observed a 10-fold increase in the recovery of colony-forming units (CFUs) from murine airways infected with succinate-stressed PAO1 compared with control PAO1 (Fig. 3, E and F). The higher bacterial load was associated with significantly greater amounts of IL-1β ($P < 0.001$) (Fig. 3G) and succinate (Fig. 3H), but no major differences in other cytokines. Significantly fewer phagocytes ($P < 0.05$) were recovered from the succinate-adapted PAO1-containing BAL (Fig. 3, I to M). This was explained by the higher percentages of dead alveolar macrophages (Fig. 3N), neutrophils (Fig. 3O), and monocytes (Fig. 3P) recovered from BAL, consistent with pyroptosis and IL-1β release induced by the high-succinate–adapted PAO1 compared with the no-succinate and low-succinate controls. Thus, adaptation to the metabolic stress induced by high succinate promotes *P. aeruginosa* survival in the airways and immunopathogenesis.

Succinate does not promote *Staphylococcus aureus* airway infection

We evaluated whether the PTEN-succinate axis also favored metabolic reprogramming of the second major CF pathogen, *S. aureus*. First, we observed that *S. aureus* infection (USA300 strain) slightly reduced PTEN expression in BAL alveolar macrophages (fig. S9, A and B) but was not associated with succinate accumulation in BAL as compared with control mice (fig. S9C). Similar findings were observed in PTEN-long–deficient mice (fig.

S9C). Second, we found that increasing concentrations of succinate reduced both *S. aureus* growth and biofilm production (fig. S9D), effects probably due to the decreased capacity of *S. aureus* to assimilate other metabolites, such as α-D-glucose, D-trehalose, D-fructose, and L-threonine (fig. S9E). Third, 500 mM succinate-stressed *S. aureus* was less able to colonize BAL and lungs in WT mice (fig. S9, F and G). Together, these results suggest that increased succinate has detrimental metabolic effects on *S. aureus* while favoring airway colonization by *P. aeruginosa*.

P. aeruginosa CF isolates display metabolic reprogramming to succinate

To confirm the clinical relevance of succinate-induced *P. aeruginosa* adaptation, we studied a collection of 17 strains isolated over 4 years from a 46-year-old patient with CF (fig. S10A) [p.Q493VfsX10/3849+10kbC>T *CFTR/CFTR*, mutations that reduce PTEN (3)]. The CF isolates fell into two major morphotypes, small colony variants and mucoid strains, both expressing 3-to 10,000-fold more antioxidant-associated *algD* than control PAO1 (fig. S10B). As expected, these morphotypes contained variable nonsynonymous mutations in clusters of small colony variant- and mucoid-specific genes, such as the *coxB* oxidase and *mucA* (Fig. 4A) (41, 42). Phenotypic analysis of antibiotic resistance, motility, pigment generation, quorum sensing, biofilm, and virulence factor production corroborated that these strains were representative of metabolically adapted *P. aeruginosa* isolates found in the CF airway, as we termed these isolates with altered expression of numerous genes in response to metabolic conditions in the airway (fig. S10, C to L) (41–46).

There were 135 genes with shared nonsynonymous mutations (table S2) identified in all genomes of the clinical isolates (table S3). Many of these mutations targeted the Entner-Doudoroff (*zwf* and *glk*), glyoxylate shunt (*aceA* and *glcB*), and TCA cycle (PA0794, *idh*, *sucA*, and *fumC1*), as well as the cyclic di-guanosine monophosphate (c–di-GMP) cascade, the master regulator of biofilm production. Representative isolates (small colony variant 686 and mucoid 605) had substantial overexpression of Entner-Doudoroff, glyoxylate shunt, and TCA cycle genes, whether mutated or not, compared with PAO1 cells. Major changes were observed in the Entner-Doudoroff–associated genes *zwf-glk* and glyoxylate shunt genes *aceA-glcB*, which were upregulated 4-to 40-fold and 20- to 80-fold, respectively (Fig. 4B). Changes in mRNA expression of TCA cycle genes were less than threefold on average with respect to PAO1. As was observed for succinate-adapted PAO1, strains selected in the CF airway favored the assimilation of α-D-glucose and its dimers, such as D-trehalose, as well as acetate and L-threonine (Fig. 4C), supporting Entner-Doudoroff and glyoxylate shunt activity (fig. S6B).

Small colony variant 686 reduced its assimilation of succinate (fig. S11), and mucoid 605 increased its succinate excretion when cultured either in acetate or in α-D-glucose (fig. S12A), likely due to increased expression of the succinate exporter *citA* (fig. S12B). As observed for in vitro–generated succinate-stressed PAO1, these clinical strains continued to grow (Fig. 4D) and produce biofilm in increasing amounts of succinate (Fig. 4E), consistent with the up-regulation of several pro-biofilm genes relative to PAO1 (Fig. 4F and fig. S12C). Reexposure of the clinical isolates to high succinate further amplified the metabolic changes seen in the Entner-Doudoroff and glyoxylate shunt pathways (Fig. 4G). These findings

suggest that the metabolic phenotype seen in *P. aeruginosa* isolates, in part, reflects adaptation to succinate in the CF airway.

CF *P. aeruginosa* isolates do not activate the airway HIF1α–succinate–IL-1β axis

The production of biofilm, as promoted by succinate exposure of the CF *P. aeruginosa* strains, is mediated by c-di-GMP, which is a signaling molecule also activated by ROS and surface contact (fig. S12C) (47). As part of the c-di-GMP cascade, the expression of several proinflammatory pathogen-associated molecular patterns (PAMPs), including LPS, is suppressed (47–49). This would, in theory, reduce the activation of immune/epithelial cells and subsequent succinate release. We noted several nonsynonymous mutations in PAMP-associated genes in all of the succinate-adapted *P. aeruginosa* isolates (Fig. 5A and table S4). Representative strains SCV 686 and mucoid 605 lost expression of *ostA* (also known as *lptD*), a protein that exposes LPS on the bacterial surface (Fig. 5B). These host-adapted strains failed to induce aerobic glycolysis in human monocytes, an expected response to LPS (Fig. 5C). Moreover, they generated less accumulation of succinate in BAL of WT mice 24 hours after infection (Fig. 5D) and failed to activate the stabilization of HIF1α in comparison to the nonadapted PAO1 control strain (Fig. 5E). As might be predicted, the host-adapted strains, either individually or in combination, stimulated significantly less IL-1β ($P < 0.001$) (Fig. 5F) as well as IL-6, TNFα, and MCP-1 proinflammatory cytokines in the murine airway (fig. S13). Instead, IL-1β accumulated intracellularly in alveolar macrophages and recruited monocytes but was not released (fig. S14). Despite preventing IL-1β secretion, CF *P. aeruginosa* isolates stimulated mitochondrial ROS production in host monocytes as did proinflammatory PAO1 (Fig. 5G).

CF *P. aeruginosa* isolates evoke an IRG1-itaconate airway immune response

The immune response to the CF isolates, namely, the induction of ROS and modest release of succinate, but lack of IL-1β release, suggested a major deregulation of the expected innate immune response to bacteria. We observed that IRG1, which produces the anti-inflammatory signaling metabolite itaconate, was significantly up-regulated in monocytes recruited into the airway by the CF strains of *P. aeruginosa* ($P < 0.0001$) (Fig. 5, H and I), as was itaconate itself ($P < 0.001$) (Fig. 5J and fig. S15). Because itaconate inhibits SDH, this increased activity could account for the modest increase in BAL succinate associated with murine infection by the CF strains (Fig. 5D). These findings indicate that in vivo adaptation to high succinate generates *P. aeruginosa* strains that retain the ability to activate mitochondrial ROS but fail to activate IL-1β release and instead promote an itaconate response in the airway cells, which suppresses inflammation (11–13, 31).

Metabolically adapted CF *P. aeruginosa* persist in the airway

The consequences of a dysfunctional immune response are evident in patients with CF as airway damage associated with recruitment of neutrophils, but a failure to eradicate infection. However, chronic *P. aeruginosa* airway infection has been difficult to model in mice, including CF mice (50, 51). Nonetheless, we were able to illustrate major differences in the pathogenicity of the CF-adapted strains compared with WT PAO1 (Fig. 6). Equivalent inocula of PAO1 and either all 17 CF strains, the small colony variant 686, or mucoid 605 isolate had very different outcomes in a C57Bl/6 model of pneumonia: We observed 100%

lethality of PAO1 at 24 hours (Fig. 6, A and B), whereas the CF strains persisted for at least 5 days (Fig. 6C). Of note, these WT mice did not have the higher concentrations of succinate that are linked to CFTR-PTEN dysfunction (Figs. 1J and 5D). Extended airway colonization by CF *P. aeruginosa* isolates was accompanied by 10-fold accumulation of more monocytes (Fig. 6D) and neutrophils (Fig. 6E) in BAL, consistent with sustained cell viability (fig. S16). Alveolar macrophages were consistently depleted by both WT and CF-adapted isolates (Fig. 6F).

Infecting *Cftr*$^{\Delta F508/\Delta F508}$ gut-corrected mice with the CF-adapted strains induced a similar accumulation of succinate (Fig. 6G) and attracted a significantly greater influx of neutrophils (Fig. 6H) and monocytes ($P < 0.05$) (Fig. 6I), but not increased numbers of alveolar macrophages (Fig. 6J), compared with the WT CFTR controls. However, despite the myeloid cell recruitment, infection was not cleared more effectively (Fig. 6, K and L).

As we predicted that deficient PTEN-CFTR interaction is a key component of the inflammatory response, we tested the ability of the *Pten*$l^{-/-}$ mice to clear infection caused by the CF-adapted strains. These CF strains did not stimulate significantly ($P > 0.05$) higher amounts of succinate in the *Pten*$l^{-/-}$ mice (Fig. 6M) and failed to activate the release of more IL-1β (Fig. 6N). The CF-adapted strains recruited significantly more neutrophils (Fig. 6O) and monocytes (Fig. 6P) ($P < 0.05$) but did not change the numbers of resident alveolar macrophages in the airways (Fig. 6Q) and, despite this immune response, phagocytes failed to eradicate infection (Fig. 6, R and S).

The similar findings in terms of succinate accumulation, immune cell recruitment, and bacterial clearance in *Cftr*$^{\Delta F508/\Delta F508}$ and *Pten*$l^{-/-}$ mice suggest that the major factor associated with chronic *P. aeruginosa* infection is increased susceptibility, that is, that the initial succinate-induced adaptation of the organisms and metabolic reprogramming enables long-term colonization of the airways. Once the organisms have adapted to succinate and other components of the CF airway, they are equally proficient in chronically infecting WT and PTEN-CFTR–deficient airways, with ongoing adaptation maintained by exposure to either endogenous or inflammation-associated succinate release.

DISCUSSION

Among the protean manifestations of CF, we demonstrated impaired mitochondrial function as a consequence of diminished PTEN activity in cells with *CFTR* mutations. This resulted in the accumulation of excess succinate in the airway, creating an environment that enhanced susceptibility to infection by *P. aeruginosa*. Among the many inadvertently inhaled pathogens, *P. aeruginosa* is programmed to induce accumulation of diverse metabolites in the airway (52) and to preferentially catabolize succinate (17–19). We found that a standard laboratory strain of *P. aeruginosa* exposed to high succinate for just 24 hours displayed substantial changes in the expression of numerous metabolic genes and had enhanced ability to infect the murine airway. CF *P. aeruginosa* isolates exhibited a similar adaptation to succinate, altering gene expression especially in the glyoxylate shunt and other metabolic pathways to limit oxidant stress through extracellular polysaccharide and biofilm production. They also down-regulated the expression of genes involved in the display of

numerous PAMPs, including LPS, that would activate immune cells and further generate succinate release and oxidants associated with its compulsory metabolism.

Despite their diverse phenotypes, the conserved metabolic changes in the CF isolates elicited a similar, ineffective immune response. In contrast to the immunostimulatory and lethal response associated with WT PAO1, the CF metabolically adapted strains failed to generate IL-1β but promoted increased recruitment of itaconate-producing myeloid cells, which did not clear infection efficiently. Thus, the CF succinate-adapted organisms persisted, protected by their succinate-induced biofilms and itaconate-suppressed immune signaling.

PAO1 grown as a laboratory isolate had properties distinct from PAO1 grown in high succinate and the CF clinical isolates. Growth in high succinate induced many of the same adaptations present in the succinate-adapted CF strains. Succinate-stressed PAO1 induced greater amounts of IL-1β, which has been shown to enhance *P. aeruginosa* airway infection (53–55). In contrast, the CF isolates, which lacked expression of PAMPs as well as having metabolic changes, failed to activate IL-1β. Thus, there are multiple factors affecting the properties of both the organisms and the nature of the host response that are ultimately reflected in the relative density of airway infection.

Our data raise questions that require several future studies. Available model systems, primary cells (PBMCs), epithelial and monocyte cell lines, and use of CF sputum–like media do not adequately replicate the complexities of the inflamed airway with metabolically active host cells and proliferating bacteria and fail to establish the relative contribution of excess succinate from the organisms versus the host. The CF models used, $Cftr^{\Delta F508/\Delta F508}$ gut-corrected and $Ptenl^{-/-}$ mice, do not entirely recapitulate the pathogenesis of *P. aeruginosa* in patients with CF, stressing the need for better experimental systems. Moreover, different *CFTR* genotypes, the heterogeneity of *P. aeruginosa* isolates, and the presence of other components of the microbiota will affect the metabolomics of the airway in patients. Our colocalization of PTEN and CFTR to the mitochondrial outer membrane requires biochemical confirmation including fractionation of mitochondrial components to demonstrate that this interaction is functional and not simply proximity with another CFTR-containing organelle. Especially intriguing is the role of PTEN in the regulation of complexes I and II, oxidative stress, and IRG1 expression in living organisms, because our studies did not determine whether the itaconate-succinate axis can be corrected in *Ptenl* and *Cftr* mutant mice by scavenging mitochondrial ROS.

Exactly how PTEN dysfunction results in this dysregulated immune response is not fully understood. PTEN deficiency affects the catabolism of isocitrate and G3P, intermediates with potential to feed the pro-oxidant complexes I and II in mitochondria. Cells lacking sufficient PTEN have increased IRG1, which inhibits complex II (SDH), as we observed. Thus, it is likely that excess ROS are derived mostly from complex I, as has been shown in tumor-derived macro-phages, PTEN-deficient fibroblast, and prostate cancer cells (56, 57). As we found that restoring PTEN corrected the oxidant stress associated with mitochondrial dysfunction in CF cells, therapeutic strategies to correct CFTR delivery to the cell membrane and, hence, its association with PTEN might also affect the itaconate-succinate axis. For many *CFTR* mutations available, correctors that improve trafficking of the mutated

protein to cell membranes, including mitochondria, may accomplish this (58–60). We predict that the cycle of *P. aeruginosa* infection, adaptation, and establishment of intractable biofilms in the airway could be mitigated by early treatment to enhance the PTEN-CFTR interaction (3) and prevent mitochondrial dysfunction and the associated alteration of the succinate/itaconate balance.

MATERIALS AND METHODS

Study design

This study was designed to evaluate how *P. aeruginosa* adapt to the CF airway to cause chronic infection. We tested our hypothesis with in vitro and in vivo experiments using laboratory and clinical isolates. The sample size per experiment is included in the figure legends. In this study, we used WT, *Ptenl*$^{-/-}$, and *Cftr*$^{\Delta F508/\Delta F508}$ gut-corrected mice as in vivo models. The number of mice used was selected based on previous studies using the same model and calculating the statistical power, considering a minimum of six mice in total pooled from at least two independent experiments. All animal experiments were performed in agreement with Institutional Animal Care and Use Committee protocol AAAR9403 at Columbia University. In vitro, we used human monocyte and epithelial cell lines, either WT, *CFTR* mutants, or *PTEN* mutants. We corrected mutant cells with viral vectors. The human samples in this study, such as CF sputum, CF blood, and *P. aeruginosa* isolates, were acquired from random adult patients who were genetically and clinically characterized as suffering from CF. Samples were acquired during routine visits to the hospital and under signed consent by each patient. Patients' personal information was never revealed to the principal researchers [Institutional Review Board (IRB) protocol AAAR1395]. Researchers only received the blood and sputum samples, and only *CFTR* mutations and whether patients were under CFTR modulator treatments were disclosed. Experiments were not performed in a blinded fashion.

Human samples

All PBMCs used in this study were obtained from blood of patients with CF and healthy volunteers under the IRB protocol AAAR1395 Columbia University. Before providing blood, all patients were explained about the project and signed a consent form included in the IRB protocol. CF sputum for succinate quantification was provided by P. Planet, Children's Hospital of Philadelphia, USA.

Mice

Six- to 8-week-old WT C57Bl/6 mice were obtained from the Jackson laboratory. *Ptenl*$^{-/-}$ mice were obtained from R. Parsons and B. Hopkins, Mount Sinai, New York. WT and *Ptenl*$^{-/-}$ mice were housed at Columbia University facilities before being used in accordance with conditions stipulated by the Institute for Comparative Medicine (AAAR9403). *Cftr*$^{\Delta F508}$ gut-corrected mice were provided by the Cystic Fibrosis Animal Core at Case Western Reserve University, bred, and maintained by C. Britto at Yale University, New Haven. Normal diet was provided before and during the infections.

Growth and biofilm of WT *P. aeruginosa* in succinate-supplemented LB media

PAO1 was grown overnight in succinate-free LB media under agitation at 37°C in a sterile tube. Then, 1 ml of bacteria was spun down, washed with cold PBS, resuspended in 1 ml of LB at an optical density (OD_{600nm}) of 1.0, and incubated in a 1/20 dilution either in the same succinate-free media or in increasing concentration of succinate added to LB (7, 15, 32, 65, 125, 250, and 500 mM) in flat-bottom 96-well plates with a final volume of 100 μl per well. Plates were incubated under agitation or static at 37°C overnight. The next day, bacterial growth (OD_{600nm}) and biofilm production (crystal violet, OD540nm) were measured.

Adaptation of WT *P. aeruginosa* and *S. aureus* to succinate in vitro

PAO1 or USA300 was grown overnight in succinate-free LB media under agitation at 37°C in a sterile tube. Then, 50 μl of bacteria was resuspended either in 3 ml in the same but fresh succinate-free media (PAO1; USA300) or in LB supplemented either with 50 mM (PAO1*; USA300*) or 500 mM succinate ($PAO1^{Succ}$; $USA300^{Succ}$). Tubes were agitated overnight at 37°C. The next day, OD_{600nm} was measured, and bacteria were prepared for the following experiments.

Infection of mice with succinate-adapted bacteria

After generating PAO1, PAO1*, and $PAO1^{Succ}$ (or USA300, USA300*, and $USA300^{Succ}$), bacteria were washed and resuspended in sterile PBS, and 10^6 CFUs (10^7 CFUs for USA300) were instilled intranasally to mice in 50 μl of PBS. Twenty-four hours later, mice were sacrificed, and BAL was collected. CFU amounts, succinate accumulation, and immune cell infiltrate were quantified in BAL. Alveolar macrophage ($CD45^+CD11b^{low/-}SiglecF^{high}CD11c^+CD193^-Ly6G^-Ly6C^-$), neutrophil ($CD45^+CD11b^{high}SiglecF^{low/-}CD11c^-MHCII^-CD193^-Ly6G^+Ly6C^{low/-}$), and monocyte ($CD45^+CD11b^{high}SiglecF^{low/-}CD11c^-MHCII^-CD193^-$ $Ly6G^-Ly6C^{low/high}$) enrichment in BAL was analyzed by flow cytometry. Total cell numbers per BAL were quantified. Cell viability was determined by using live/dead DAPI staining (Life Technologies).

Mouse infection experiments with *P. aeruginosa* isolates

When indicated, anesthetized WT C57Bl/6, *Ptenl*$^{-/-}$, or *Cftr*$^{\Delta F508}$ gut-corrected mice were infected intranasally with either 1×10^7 CFUs of laboratory strain PAO1, a total 1×10^7 CFU mix of all 17 isolates (equal parts—5.9×10^5 for each), 1×10^7 CFUs of SCV variant 686, 1×10^7 CFUs of mucoid strain 605, or a total 1×10^7 CFU mix of both 686 + 605 (5×10^6 of each). Mice viability was monitored. In addition, 24 hours/48 hours after infection (when indicated), lung and BAL tissues were collected and analyzed by Western blot and enzyme-linked immunosorbent assay for IL-1β and other cytokines. BAL and lung cells were also analyzed by flow cytometry to evaluate immune cell recruitment as well as intracellular IRG1 protein levels. Succinate was quantified in BALs using a colorimetric assay.

Statistical analyses

All analyses and graphs were performed using the GraphPad Prism 7a software. Differences in the mean between two groups were analyzed using Student's *t* test or ANOVA for normally distributed data and Mann-Whitney or Kruskal-Wallis test otherwise. To compare means between more than two groups, we performed a one-way ANOVA with a multiple posteriori comparison (Tukey or Dunnett). When studying two or more group along time, data were analyzed using a two-way ANOVA with multiple posteriori comparison (Tukey). Mouse survival was analyzed using the Kaplan-Meier test. $P < 0.05$ (two sided) was considered significant.

Additional Materials and Methods can be found in the Supplementary Materials.

Supplementary Material

Refer to Web version on PubMed Central for supplementary material.

Acknowledgments:

We thank I. Lewis and R. Groves for their support with the metabolomics studies. Mutant mice homozygous for the CF-causing mutation *Cftr*$^{\Delta F508/\Delta F508}$ expressing normal human CFTR protein under control of the rat gut FABP promoter [C57Bl/6 *Cftr*$^{tm1Kth/TgN(FABPCFTR)\#Jaw/Cwr}$] were obtained from the CF Animal Core at Case Western Reserve University and bred in our laboratory. *Pten*$l^{-/-}$ mice and *PTEN*$^{-/-}$ cell lines were provided by R. Parsons and B. Hopkins, Mount Sinai, New York.

Funding: A.P. was supported by NIH 1R35HL135800 and by Integrating Special Populations (ISP) Resource, CTSA, Columbia University (GG011557–26); S.A.R. by a CFF Postdoctoral fellowship RIQUEL 17F0/PG008837; C.L. by S. B. Postdoctoral contract CD15/00125 and M-AES mobility grant MV16/00053; and P.P. by the Pediatric Infectious Diseases Society–St. Jude Award, Thrasher Early Investigator Award (PG005871), Clinical Doris Duke Clinical Scientist Development Award (#2012060), Louis V. Gerstner Scholar Award, and CFF Pilot Grant (PLANET16I). This publication was supported by the NCATS-NIH (UL1TR001873) and ISCIII (FIS PI16/01381) and was performed in the CCTI Flow Cytometry Core at CUMC, NIH (S10RR027050).

REFERENCES AND NOTES

1. Luciani A, Villella VR, Esposito S, Brunetti-Pierri N, Medina D, Settembre C, Gavina M, Pulze L, Giardino I, Pettoello-Mantovani M, D'Apolito M, Guido S, Masliah E, Spencer B, Quaratino S, Raia V, Ballabio A, Maiuri L, Defective CFTR induces aggresome formation and lung inflammation in cystic fibrosis through ROS-mediated autophagy inhibition. Nat. Cell Biol 12, 863–875 (2010). [PubMed: 20711182]
2. Elborn JS, Cystic fibrosis. Lancet 388, 2519–2531 (2016). [PubMed: 27140670]
3. Riquelme SA, Hopkins BD, Wolfe AL, DiMango E, Kitur K, Parsons R, Prince A, Cystic fibrosis transmembrane conductance regulator attaches tumor suppressor PTEN to the Membrane and Promotes Anti *Pseudomonas aeruginosa* immunity. Immunity 47, 1169–1181.e7 (2017). [PubMed: 29246444]
4. Ortega-Molina A, Serrano M, PTEN in cancer, metabolism, and aging. Trends Endocrinol. Metab 24, 184–189 (2013). [PubMed: 23245767]
5. Blouin M-J, Zhao Y, Zakikhani M, Algire C, Piura E, Pollak M, Loss of function of PTEN alters the relationship between glucose concentration and cell proliferation, increases glycolysis, and sensitizes cells to 2-deoxyglucose. Cancer Lett 289, 246–253 (2010). [PubMed: 19744772]
6. Bankoglu EE, Tschopp O, Schmitt J, Burkard P, Jahn D, Geier A, Stopper H, Role of PTEN in oxidative stress and DNA damage in the liver of whole-body *Pten* haplodeficient mice. PLOS ONE 11, e0166956 (2016). [PubMed: 27893783]
7. Everts B, Amiel E, Huang SC-C, Smith AM, Chang C-H, Lam WY, Redmann V, Freitas TC, Blagih J, van der Windt GJW, Artyomov MN, Jones RG, Pearce EL, Pearce EJ, TLR-driven early

glycolytic reprogramming via the kinases TBK1-IKKε supports the anabolic demands of dendritic cell activation. Nat. Immunol 15, 323–332 (2014). [PubMed: 24562310]

8. Denko NC, Hypoxia, HIF1 and glucose metabolism in the solid tumour. Nat. Rev. Cancer 8, 705–713 (2008). [PubMed: 19143055]
9. Tannahill GM, Curtis AM, Adamik J, Palsson-McDermott EM, McGettrick AF, Goel G, Frezza C, Bernard NJ, Kelly B, Foley NH, Zheng L, Gardet A, Tong Z, Jany SS, Corr SC, Haneklaus M, Caffrey BE, Pierce K, Walmsley S, Beasley FC, Cummins E, Nizet V, Whyte M, Taylor CT, Lin H, Masters SL, Gottlieb E, Kelly VP, Clish C, Auron PE, Xavier RJ, O'Neill LAJ, Succinate is an inflammatory signal that induces IL-1β through HIF-1α. Nature 496, 238–242 (2013). [PubMed: 23535595]
10. Corcoran SE, O'Neill LAJ, HIF1α and metabolic reprogramming in inflammation. J. Clin. Invest 126, 3699–3707 (2016). [PubMed: 27571407]
11. Murphy MP, O'Neill LAJ, Krebs cycle reimagined: The emerging roles of succinate and itaconate as signal transducers. Cell 174, 780–784 (2018). [PubMed: 30096309]
12. Lampropoulou V, Sergushichev A, Bambouskova M, Nair S, Vincent EE, Loginicheva E, Cervantes-Barragan L, Ma X, Huang SC-C, Griss T, Weinheimer CJ, Khader S, Randolph GJ, Pearce EJ, Jones RG, Diwan A, Diamond MS, Artyomov MN, Itaconate links inhibition of succinate dehydrogenase with macrophage metabolic remodeling and regulation of inflammation. Cell Metab 24, 158–166 (2016). [PubMed: 27374498]
13. Cordes T, Wallace M, Michelucci A, Divakaruni AS, Sapcariu SC, Sousa C, Koseki H, Cabrales P, Murphy AN, Hiller K, Metallo CM, Immunoresponsive Gene 1 and itaconate inhibit succinate dehydrogenase to modulate intracellular succinate levels. J. Biol. Chem 291, 14274–14284 (2016). [PubMed: 27189937]
14. Littlewood-Evans A, Sarret S, Apfel V, Loesle P, Dawson J, Zhang J, Muller A, Tigani B, Kneuer R, Patel S, Valeaux S, Gommermann N, Rubic-Schneider T, Junt T, Carballido JM, GPR91 senses extracellular succinate released from inflammatory macrophages and exacerbates rheumatoid arthritis. J. Exp. Med 213, 1655–1662 (2016). [PubMed: 27481132]
15. Li Y, He L, Zeng N, Sahu D, Cadenas E, Shearn C, Li W, Stiles BL, Phosphatase and tensin homolog deleted on chromosome 10 (PTEN) signaling regulates mitochondrial biogenesis and respiration via estrogen-related receptor α (ERRα). J. Biol. Chem 288, 25007–25024 (2013). [PubMed: 23836899]
16. Hobert JA, Mester JL, Moline J, Eng C, Elevated plasma succinate in *PTEN*, *SDHB*, and *SDHD* mutation–positive individuals. Genet. Med 14, 616–619 (2012). [PubMed: 22261759]
17. Görke B, Stülke J, Carbon catabolite repression in bacteria: Many ways to make the most out of nutrients. Nat. Rev. Microbiol 6, 613–624 (2008). [PubMed: 18628769]
18. Rojo F, Carbon catabolite repression in *Pseudomonas*: Optimizing metabolic versatility and interactions with the environment. FEMS Microbiol. Rev 34, 658–684 (2010). [PubMed: 20412307]
19. Wolff JA, MacGregor CH, Eisenberg RC, Phibbs PV Jr., Isolation and characterization of catabolite repression control mutants of *Pseudomonas aeruginosa* PAO. J. Bacteriol 173, 4700–4706 (1991). [PubMed: 1906870]
20. O'Toole GA, Gibbs KA, Hager PW, Phibbs PV Jr., Kolter R, The global carbon metabolism regulator Crc is a component of a signal transduction pathway required for biofilm development by *Pseudomonas aeruginosa*. J. Bacteriol 182, 425–431 (2000). [PubMed: 10629189]
21. Tatke G, Kumari H, Silva-Herzog E, Ramirez L, Mathee K, *Pseudomonas aeruginosa* MifS-MifR two-component system is specific for α-ketoglutarate utilization. PLOS ONE 10, e0129629 (2015). [PubMed: 26114434]
22. Park J-H, Ku HJ, Lee JH, Park J-W, Disruption of IDH2 attenuates lipopolysaccharide-induced inflammation and lung injury in an α-ketoglutarate-dependent manner. Biochem. Biophys. Res. Commun 503, 798–802 (2018). [PubMed: 29913148]
23. Friedrich M, Bunse L, Wick W, Platten M, Perspectives of immunotherapy in isocitrate dehydrogenase-mutant gliomas. Curr. Opin. Oncol 30, 368–374 (2018). [PubMed: 30102604]
24. Vinogradov AD, Grivennikova VG, Oxidation of NADH and ROS production by respiratory complex I. Biochim. Biophys. Acta 1857, 863–871 (2016). [PubMed: 26571336]

25. Kiefmann M, Tank S, Keller P, Börnchen C, Rinnenthal JL, Tritt M-O, Schulte-Uentrop LS, Olotu C, Goetz AE, Kiefmann R, IDH3 mediates apoptosis of alveolar epithelial cells type 2 due to mitochondrial Ca2+ uptake during hypocapnia. Cell Death Dis 8, e3005 (2017). [PubMed: 28837149]
26. Mráček T, Holzerová E, Drahota Z, Kovářová N, Vrbacký M, Ješina P, Houštěk J, ROS generation and multiple forms of mammalian mitochondrial glycerol-3-phosphate dehydrogenase. Biochim. Biophys. Acta 1837, 98–111 (2014). [PubMed: 23999537]
27. Mills EL, Kelly B, Logan A, Costa ASH, Varma M, Bryant CE, Tourlomousis P, Däbritz JHM, Gottlieb E, Latorre I, Corr SC, McManus G, Ryan D, Jacobs HT, Szibor M, Xavier RJ, Braun T, Frezza C, Murphy MP, O'Neill LA, Succinate Dehydrogenase Supports Metabolic Repurposing of Mitochondria to Drive Inflammatory Macrophages. Cell 167, 457–470.e13 (2016). [PubMed: 27667687]
28. Hopkins BD, Fine B, Steinbach N, Dendy M, Rapp Z, Shaw J, Pappas K, Yu JS, Hodakoski C, Mense S, Klein J, Pegno S, Sulis ML, Goldstein H, Amendolara B, Lei L, Maurer M, Bruce J, Canoll P, Hibshoosh H, Parsons R, A secreted PTEN phosphatase that enters cells to alter signaling and survival. Science 341, 399–402 (2013). [PubMed: 23744781]
29. Liang H, He S, Yang J, Jia X, Wang P, Chen X, Zhang Z, Zou X, McNutt MA, Shen WH, Yin Y, PTENα, a PTEN isoform translated through alternative initiation, regulates mitochondrial function and energy metabolism. Cell Metab 19, 836–848 (2014). [PubMed: 24768297]
30. Velsor LW, Kariya C, Kachadourian R, Day BJ, Mitochondrial oxidative stress in the lungs of cystic fibrosis transmembrane conductance regulator protein mutant mice. Am. J. Respir. Cell Mol. Biol 35, 579–586 (2006). [PubMed: 16763223]
31. Mills EL, Ryan DG, Prag HA, Dikovskaya D, Menon D, Zaslona Z, Jedrychowski MP, Costa ASH, Higgins M, Hams E, Szpyt J, Runtsch MC, King MS, McGouran JF, Fischer R, Kessler BM, McGettrick AF, Hughes MM, Carroll RG, Booty LM, Knatko EV, Meakin PJ, Ashford MLJ, Modis LK, Brunori G, Sévin DC, Fallon PG, Caldwell ST, Kunji ERS, Chouchani ET, Frezza C, Dinkova-Kostova AT, Hartley RC, Murphy MP, O'Neill LA, Itaconate is an anti-inflammatory metabolite that activates Nrf2 via alkylation of KEAP1. Nature 556, 113–117 (2018). [PubMed: 29590092]
32. Lemire J, Alhasawi A, Appanna VP, Tharmalingam S, Appanna VD, Metabolic defence against oxidative stress: The road less travelled so far. J. Appl. Microbiol 123, 798–809 (2017). [PubMed: 28609580]
33. Kirchner S, Fothergill JL, Wright EA, James CE, Mowat E, Winstanley C, Use of artificial sputum medium to test antibiotic efficacy against *Pseudomonas aeruginosa* in conditions more relevant to the cystic fibrosis lung. J. Vis. Exp 5, e3857 (2012).
34. Ahn S, Jung J, Jang I-A, Madsen EL, Park W, Role of glyoxylate shunt in oxidative stress response. J. Biol. Chem 291, 11928–11938 (2016). [PubMed: 27036942]
35. Meylan S, Porter CBM, Yang JH, Belenky P, Gutierrez A, Lobritz MA, Park J, Kim SH, Moskowitz SM, Collins JJ, Carbon sources tune antibiotic susceptibility in *Pseudomonas aeruginosa* via tricarboxylic acid cycle control. Cell Chem. Biol 24, 195–206 (2017). [PubMed: 28111098]
36. Meylan S, Andrews IW, Collins JJ, Targeting antibiotic tolerance, pathogen by pathogen. Cell 172, 1228–1238 (2018). [PubMed: 29522744]
37. Hentzer M, Teitzel GM, Balzer GJ, Heydorn A, Molin S, Givskov M, Parsek MR, Alginate overproduction affects *Pseudomonas aeruginosa* biofilm structure and function. J. Bacteriol 183, 5395–5401 (2001). [PubMed: 11514525]
38. May TB, Shinabarger D, Maharaj R, Kato J, Chu L, DeVault JD, Roychoudhury S, Zielinski NA, Berry A, Rothmel RK, Alginate synthesis by *Pseudomonas aeruginosa*: A key pathogenic factor in chronic pulmonary infections of cystic fibrosis patients. Clin. Microbiol. Rev 4, 191–206 (1991). [PubMed: 1906371]
39. Simpson JA, Smith SE, Dean RT, Scavenging by alginate of free radicals released by macrophages. Free Radic. Biol. Med 6, 347–353 (1989). [PubMed: 2540067]
40. Wozniak DJ, Wyckoff TJO, Starkey M, Keyser R, Azadi P, O'Toole GA, Parsek MR, Alginate is not a significant component of the extracellular polysaccharide matrix of PA14 and PAO1

Pseudomonas aeruginosa biofilms. Proc. Natl. Acad. Sci. U.S.A 100, 7907–7912 (2003). [PubMed: 12810959]

41. Starkey M, Hickman JH, Ma L, Zhang N, de Long S, Hinz A, Palacios S, Manoil C, Kirisits MJ, Starner TD, Wozniak DJ, Harwood CS, Parsek MR, *Pseudomonas aeruginosa* rugose small-colony variants have adaptations that likely promote persistence in the cystic fibrosis lung. J. Bacteriol 191, 3492–3503 (2009). [PubMed: 19329647]
42. Winstanley C, O'Brien S, Brockhurst MA, *Pseudomonas aeruginosa* evolutionary adaptation and diversification in cystic fibrosis chronic lung infections. Trends Microbiol 24, 327–337 (2016). [PubMed: 26946977]
43. Marvig RL, Sommer LM, Molin S, Johansen HK, Convergent evolution and adaptation of *Pseudomonas aeruginosa* within patients with cystic fibrosis. Nat. Genet 47, 57–64 (2015). [PubMed: 25401299]
44. Lozano C, Azcona-Gutierrez JM, Van Bambeke F, Sáenz Y, Great phenotypic and genetic variation among successive chronic *Pseudomonas aeruginosa* from a cystic fibrosis patient. PLOS ONE 13, e0204167 (2018). [PubMed: 30212579]
45. Janjua HA, Segata N, Bernabò P, Tamburini S, Ellen A, Jousson O, Clinical populations of *Pseudomonas aeruginosa* isolated from acute infections show a wide virulence range partially correlated with population structure and virulence gene expression. Microbiology 158, 2089–2098 (2012). [PubMed: 22556359]
46. McCaughey G, Gilpin DF, Schneiders T, Hoffman LR, McKevitt M, Elborn JS, Tunney MM, Fosfomycin and tobramycin in combination downregulate nitrate reductase genes *narG* and *narH*, resulting in increased activity against *Pseudomonas aeruginosa* under anaerobic conditions. Antimicrob. Agents Chemother 57, 5406–5414 (2013). [PubMed: 23959314]
47. Valentini M, Filloux A, Biofilms and Cyclic di-GMP (c-di-GMP) signaling: Lessons from *Pseudomonas aeruginosa* and Other Bacteria. J. Biol. Chem 291, 12547–12555 (2016). [PubMed: 27129226]
48. McCarthy RR, Mazon-Moya MJ, Moscoso JA, Hao Y, Lam JS, Bordi C, Mostowy S, Filloux A, Cyclic-di-GMP regulates lipopolysaccharide modification and contributes to *Pseudomonas aeruginosa* immune evasion. Nat. Microbiol 2, 17027 (2017). [PubMed: 28263305]
49. Chua SL, Ding Y, Liu Y, Cai Z, Zhou J, Swarup S, Drautz-Moses DI, Schuster SC, Kjelleberg S, Givskov M, Yang L, Reactive oxygen species drive evolution of pro-biofilm variants in pathogens by modulating cyclic-di-GMP levels. Open Biol 6, 160162 (2016). [PubMed: 27881736]
50. Lavelle GM, White MM, Browne N, McElvaney NG, Reeves EP, Animal models of cystic fibrosis pathology: Phenotypic parallels and divergences. Biomed. Res. Int 2016, 5258727 (2016). [PubMed: 27340661]
51. Yan Z, Stewart ZA, Sinn PL, Olsen JC, Hu J, McCray PB Jr., Engelhardt JF, Ferret and pig models of cystic fibrosis: Prospects and promise for gene therapy. Hum. Gene. Ther. Clin. Dev 26, 38–49 (2015). [PubMed: 25675143]
52. LeGouellec A, Moyne O, Meynet E, Toussaint B, Fauvelle F, High-resolution magic angle spinning NMR-based metabolomics revealing metabolic changes in lung of mice infected with *P. aeruginosa* consistent with the degree of disease severity. J. Proteome Res 17, 3409–3417 (2018). [PubMed: 30129763]
53. Cohen TS, Prince AS, Activation of inflammasome signaling mediates pathology of acute *P. aeruginosa* pneumonia. J. Clin. Invest 123, 1630–1637 (2013). [PubMed: 23478406]
54. Schultz MJ, Rijneveld AW, Florquin S, Edwards CK, Dinarello CA, van der Poll T, Role of interleukin-1 in the pulmonary immune response during *Pseudomonas aeruginosa* pneumonia. Am. J. Physiol. Lung Cell. Mol. Physiol 282, L285–L290 (2002). [PubMed: 11792633]
55. Iannitti RG, Napolioni V, Oikonomou V, De Luca A, Galosi C, Pariano M, Massi-Benedetti C, Borghi M, Puccetti M, Lucidi V, Colombo C, Fiscarelli E, Lass-Flörl C, Majo F, Cariani L, Russo M, Porcaro L, Ricciotti G, Ellemunter H, Ratclif L, de Benedictis FM, Talesa VN, Dinarello CA, van de Veerdonk FL, Romani L, IL-1 receptor antagonist ameliorates inflammasome-dependent inflammation in murine and human cystic fibrosis. Nat. Commun 7, 10791 (2016). [PubMed: 26972847]

56. Naguib A, Mathew G, Reczek CR, Watrud K, Ambrico A, Herzka T, Salas IC, Lee MF, El-Amine N, Zheng W, Di Francesco ME, Marszalek JR, Pappin DJ, Chandel NS, Trotman LC, Mitochondrial complex I inhibitors expose a vulnerability for selective killing of *Pten*-null cells. Cell Rep 23, 58–67 (2018). [PubMed: 29617673]

57. Weiss JM, Davies LC, Karwan M, Ileva L, Ozaki MK, Cheng RYS, Ridnour LA, Annunziata CM, Wink DA, McVicar DW, Itaconic acid mediates crosstalk between macrophage metabolism and peritoneal tumors. J. Clin. Invest 128, 3794–3805 (2018). [PubMed: 29920191]

58. Mayer-Hamblett N, Boyle M, VanDevanter D, Advancing clinical development pathways for new CFTR modulators in cystic fibrosis. Thorax 71, 454–461 (2016). [PubMed: 26903594]

59. Grasemann H, CFTR modulator therapy for cystic fibrosis. N. Engl. J. Med 377, 2085–2088 (2017). [PubMed: 29099349]

60. Harutyunyan M, Huang Y, Mun KS, Yang F, Arora K, Naren AP, Personalized medicine in CF: from modulator development to therapy for cystic fibrosis patients with rare CFTR mutations. Am. J. Physiol. Lung Cell. Mol. Physiol 314, L529–L543 (2018). [PubMed: 29351449]

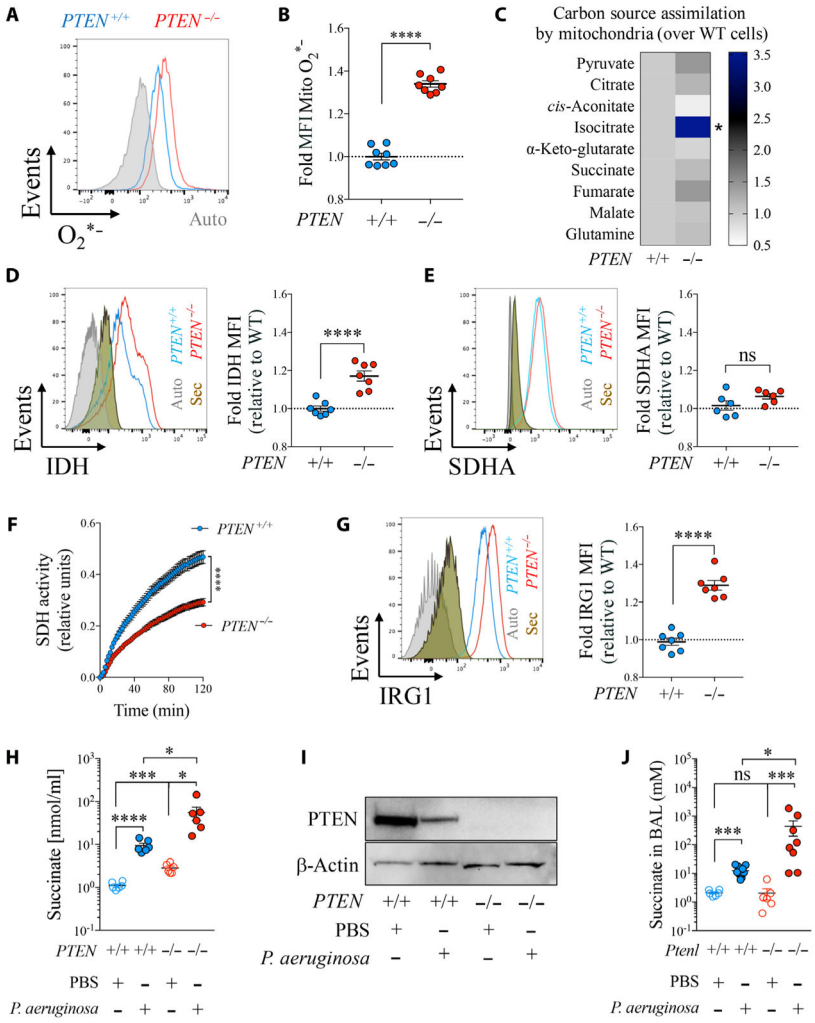

Fig. 1. PTEN regulates the ROS-IRG1-succinate mitochondrial axis.

(**A** to **I**) *PTEN*$^{+/+}$ and *PTEN*$^{-/-}$ HTC116 human epithelial cells were analyzed for (A and B) mitochondrial $O_2{}^{*-}$ production ($n = 3$). (C) Assimilation by mitochondria of different carbon sources that feed the TCA cycle ($n = 6$). (D and E) Intracellular IDH and SDHA ($n = 3$). (F) Total SDH activity in protein extracts ($n = 3$). (G) Intracellular IRG1 ($n = 3$). (H) Succinate in the supernatant of cells infected or not with *P. aeruginosa* ($n = 3$). (I) PTEN expression before and after infection with *P. aeruginosa* (PAO1). (**J**) Succinate in the airway fluid of WT or PTEN-long–deficient mice (*Ptenl*$^{-/-}$) infected for 24 hours or not with *P. aeruginosa* (6 to 11 mice per group pooled from $n = 3$). Autofluorescence (gray) and secondary antibody staining alone (brown) for flow cytometry are shown in histograms. Data are shown as mean ± SEM. (B), (D), (E), and (G) were analyzed by Student's *t* test; (F) was analyzed by two-way analysis of variance (ANOVA); and (H) and (J) were analyzed by one-way ANOVA. ****$P < 0.0001$; ***$P < 0.001$; *$P < 0.05$; ns, nonsignificant. MFI, mean fluorescence intensity.

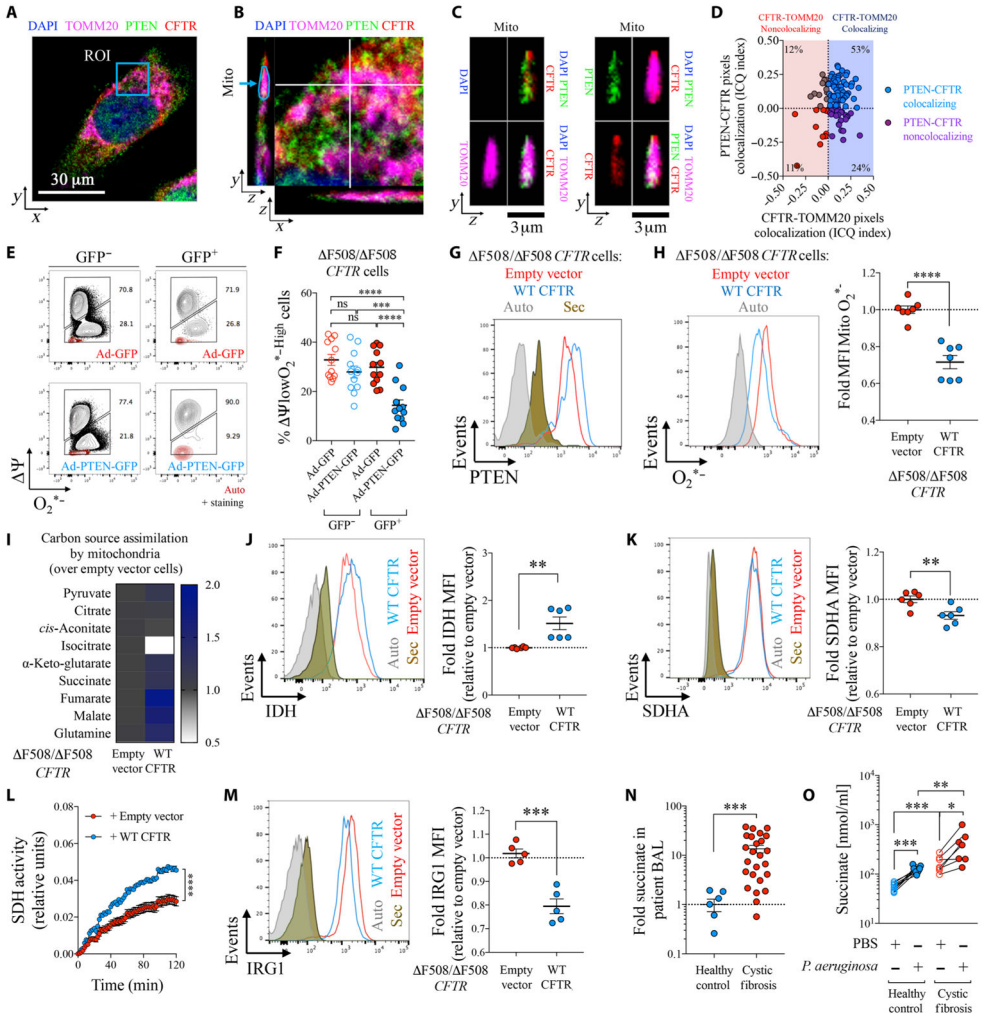

Fig. 2. PTEN correction in dysfunctional CF mitochondria restores the ROS-IRG1-succinate balance.

(**A**) A 16HBE epithelial cell stained by confocal microscopy for PTEN (green), CFTR (red), TOMM20 (magenta), and nuclei (blue). One random focal plane is shown. ROI, region of interest. (**B**) Zoom-in view of ROI shown in (A). A focal plane was analyzed in the (*y*, *z*) and (*x*, *z*) dimensions. "Mito" corresponds to a random mitochondrion captured in the (*y*, *z*) focal plane. (**C**) Zoom-in view on the mitochondrion from (B). Combined color channels are shown. (**D**) Colocalization between CFTR and TOMM20 (*x* axis) and PTEN and CFTR (*y* axis) inside mitochondria as in (B). Co-localization was measured by Intensity Correlation Quotient (ICQ) for at least 100 mitochondria from at least $n = 5$ different cells. (**E** and **F**) Percentage of $\Delta\Psi low O_2{}^{*-High}$ in human ΔF508/ΔF508 *CFTR* cells infected with a PTEN-GFP or GFP-coding adenovirus (Ad). Transduced (GFP^+) or nontransduced (GFP^-) cells are shown ($n = 3$). (**G** to **M**) ΔF508/ΔF508 *CFTR* cells corrected with a WT CFTR–expressing lentivirus or treated with an empty vector were analyzed for (G) intracellular PTEN, (H) mitochondrial ROS ($O_2{}^{*-}$) ($n = 3$), (I) mitochondrial assimilation of specific TCA cycle intermediates ($n = 6$), (J and K) intracellular IDH and SDHA ($n = 3$), (L) total SDH activity in protein extracts ($n = 2$), and (M) intracellular IRG1($n = 3$). (**N**) Fold change in succinate

in CF relative to control airways ($n = 7$ for HP and $n = 25$ for CF). (**O**) Succinate in supernatants of PBMCs from CF or controls with or without *P. aeruginosa* infection ($n = 7$ to 9). Histograms show autofluorescence (gray) and staining with secondary antibody alone (brown) for flow cytometry. Data are shown as means ± SEM. (H), (J), (K), (M), and (N) were analyzed by Student's *t* test; (L) was analyzed by two-way ANOVA; and (F) and (O) were analyzed by one-way ANOVA. ****$P < 0.0001$; ***$P < 0.001$; **$P < 0.01$; *$P < 0.05$.

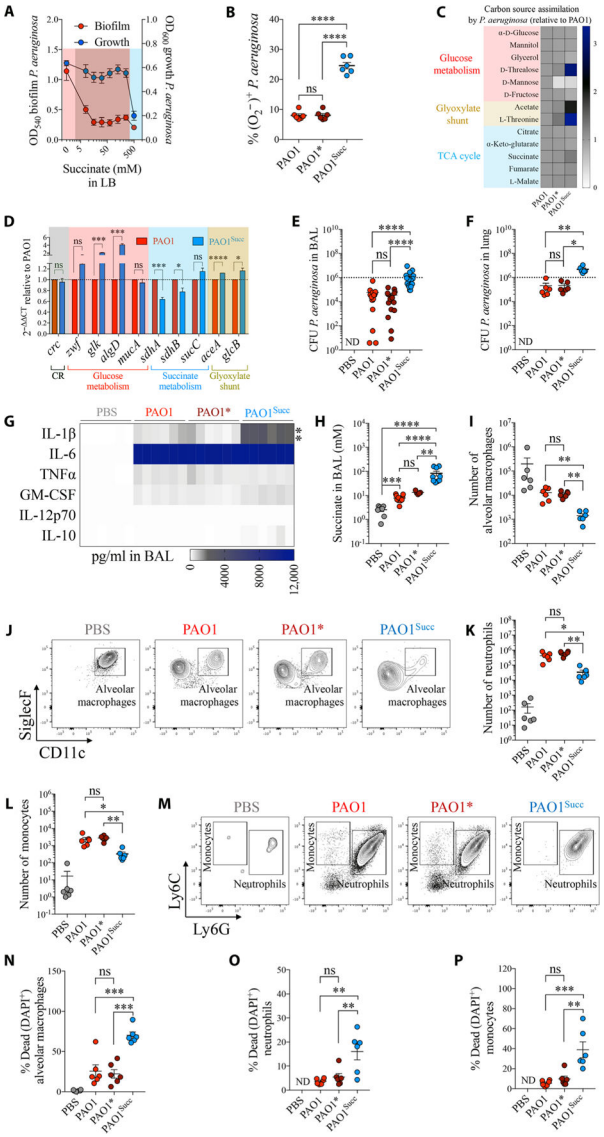

Fig. 3. Succinate promotes metabolic adaptation of *P. aeruginosa* and airway infection.
(**A**) Growth and biofilm of WT *P. aeruginosa* (PAO1) in increasing concentrations of succinate in LB media ($n = 3$). Pink, no succinate; red, 50 to 250 mM succinate; blue, 500 mM succinate. (**B**) Intracellular $O_2{}^{*-}2$ (ROS) in *P. aeruginosa* by succinate (PAO1, no succinate; PAO1*, 50 mM succinate; PAO1^{Succ}, 500 mM succinate) ($n = 3$). (**C**) Relative single-carbon source assimilation by PAO1 (control), PAO1*, and PAO1^{Succ} ($n = 3$). (**D**) mRNA expression relative to PAO1 for different metabolic pathways ($n = 3$). Mice were either infected with PAO1, PAO1*, or PAO1^{Succ} or treated with phosphate-buffered saline (PBS). Twenty-four hours later, the following were analyzed in mouse airways: (**E** and **F**) CFU found in BAL and lungs (6 to 18 mice per group pooled from $n = 3$), (**G**) heatmap of different cytokines accumulated in BAL (6 mice per group pooled from $n = 3$), (**H**) succinate accumulated in BAL (5 to 11 mice per group pooled from $n = 3$), (**I** and **J**) number and density plots of viable alveolar macrophages in BAL (6 mice per group pooled from $n = 3$), (**K** to **M**) number and density plots of viable neutrophils and monocytes in BAL (6 mice per

group pooled from $n = 3$), and (**N** to **P**) percentage of dead cells in BAL (6 mice per group pooled from $n = 3$). Data are shown as means ± SEM. ****$P < 0.0001$; ***$P < 0.001$; **$P < 0.01$; *$P < 0.05$; one-way ANOVA. ND, not detected. TNFα, tumor necrosis factor–α; GM-CSF, granulocyte-macrophage colony-stimulating factor; DAPI, 4′,6-diamidino-2-phenylindole.

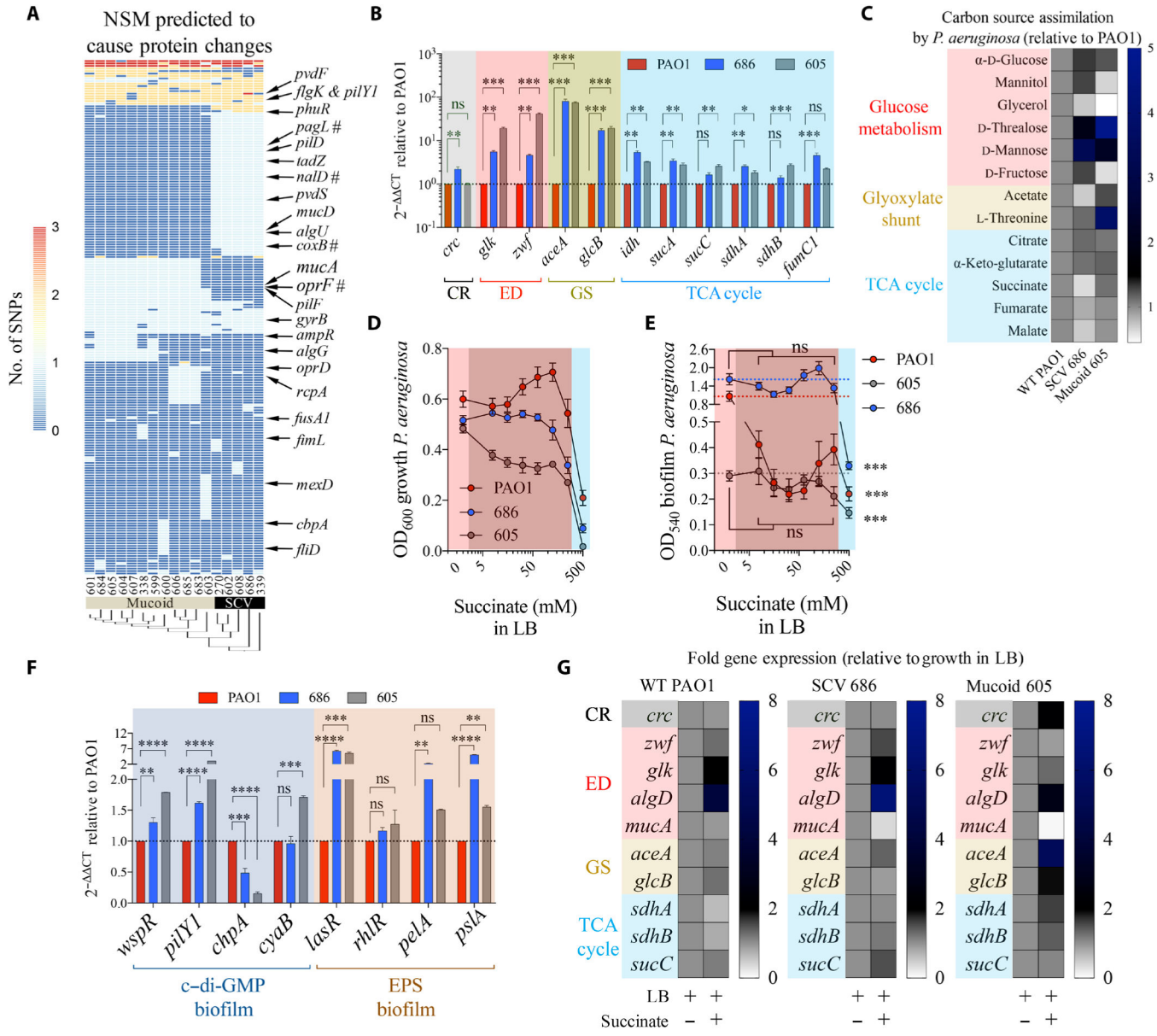

Fig. 4. Metabolism of *P. aeruginosa* isolates is consistent with adaptation to succinate.

(**A**) Nonsynonymous mutations (NSM) in 17 *P. aeruginosa* isolates (SCV and mucoid variants) compared with PAO1 control. #: stop codon mutations. (**B**) Fold mRNA expression relative to PAO1 for selected metabolic genes in SCV 686 and mucoid 605 ($n = 3$). (**C**) Relative single-carbon source assimilation for PAO1, SCV 686, and mucoid 605 strains ($n = 6$). (**D**) Bacterial final point growth in increasing concentrations of succinate in LB ($n = 3$). (**E**) Bacterial biofilm in increasing concentrations of succinate in LB ($n = 3$). (**F**) Relative mRNA expression against control PAO1 by quantitative reverse transcription polymerase chain reaction (qRT-PCR) of genes that regulate c-di-GMP and EPS required to produce biofilm ($n = 3$). (**G**) Regulation of metabolic genes by succinate in *P. aeruginosa* SCV 686 and mucoid 605 clinical isolates ($n = 3$). Data are shown as means ± SEM. (B and F) One-

way ANOVA; (D and E) two-way ANOVA. ****$P < 0.0001$; ***$P < 0.001$; **$P < 0.01$; *$P < 0.05$.

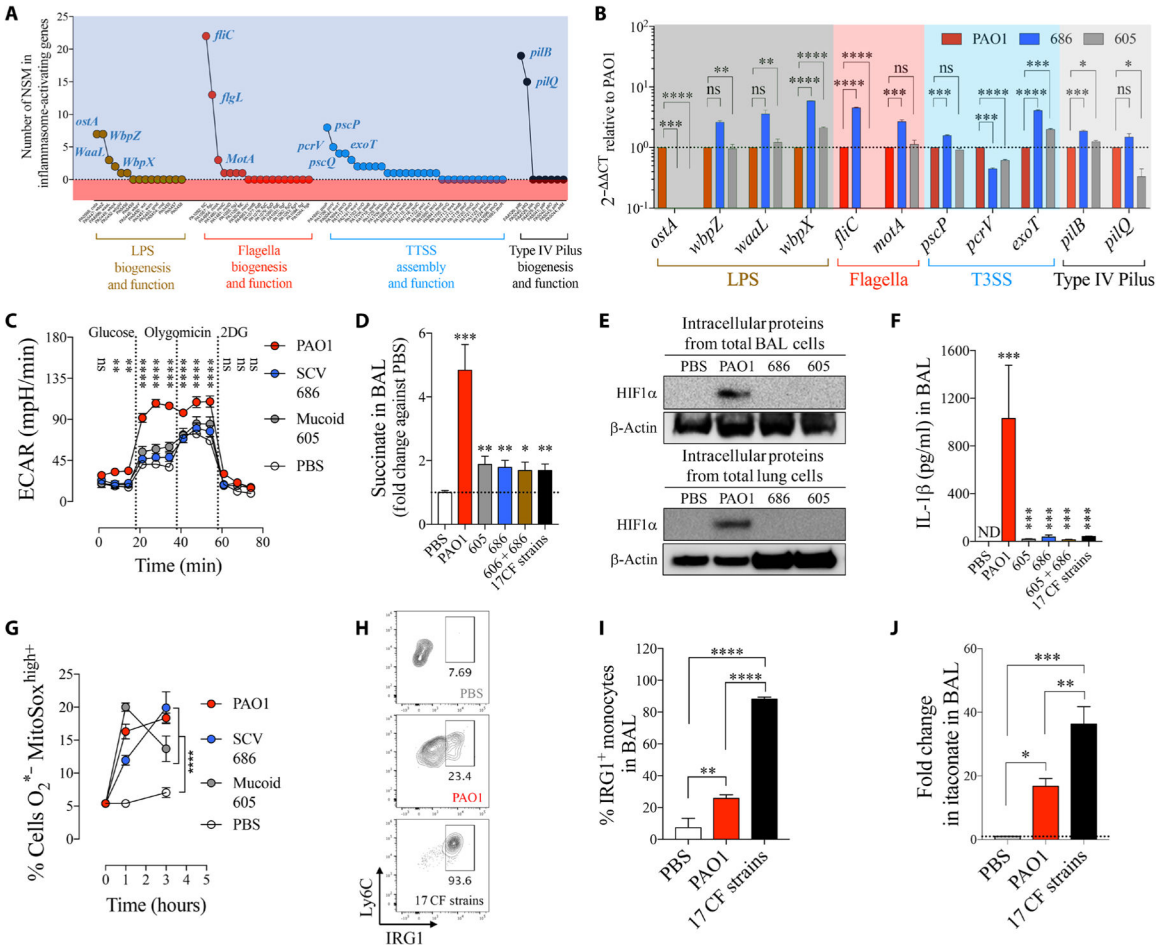

Fig. 5. Succinate-adapted *P. aeruginosa* isolates evoke an inefficient IRG1-itaconate–mediated immune response.

(**A**) Number of nonsynonymous mutations found in all *P. aeruginosa* isolates in PAMPs known to activate the IL-1β–HIF1α–succinate axis (inflammasome). (**B**) Fold mRNA expression relative to PAO1 for PAMPs with the most NSM in SCV 686 and mucoid 605 ($n = 3$). (**C**) Extracellular acidification rate (ECAR) in human monocytes treated either with PBS, PAO1, SCV 686, or mucoid 605 strain. Increased ECAR is an expected response to augmented glycolysis ($n = 2$). (**D**) Fold change in succinate in airways of WT mice treated for 24 hours with PBS, PAO1, with a single or a mixture of *P. aeruginosa* clinical isolates (six to seven mice per group pooled from $n = 3$). (**E**) BAL and lung HIF1α levels from total intracellular protein of mice infected as in (D). (**F**) IL-1β in airways of mice treated as in (D) (six to seven mice per group pooled from $n = 3$). (**G**) Mitochondrial ROS in human THP-1 cell induced by PAO1 or CF *P. aeruginosa* isolates ($n = 3$). (**H** and **I**) IRG1$^+$ monocytes (six mice per group pooled from $n = 2$) and (**J**) itaconate in BAL of PBS-, PAO1-, or 17 CF strains–treated mice (four mice per group pooled from $n = 2$). Data are shown as means ± SEM. (B), (D), (F), (I), and (J) were analyzed by one-way ANOVA; and (C) and (G) were analyzed by two-way ANOVA. ****$P < 0.0001$; ***$P < 0.001$; **$P < 0.01$; *$P < 0.05$.

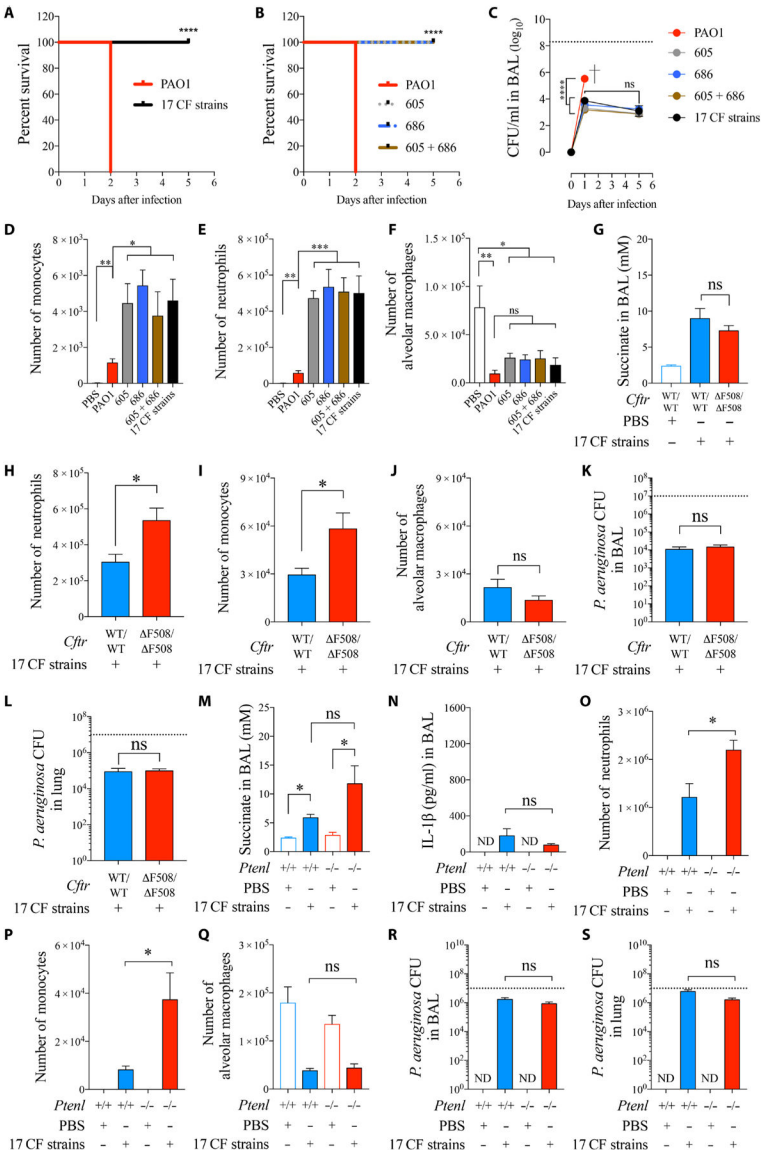

Fig. 6. CF *P. aeruginosa* isolates persist in the airway.

C57Bl/6 WT mice were intranasally infected with 10^7 CFUs of either PAO1, single CF isolates, a mixture of two, or all 17 strains together. (**A** and **B**) Mouse survival (five mice per group pooled from $n = 2$). (**C**) *P. aeruginosa* burden in BAL (four to seven mice per group pooled from $n = 3$). (**D** to **F**) Monocytes, neutrophils, and alveolar macrophages found in BAL 24 hours after infection (four to six mice per group pooled from $n = 3$). *Cftr*$^{\Delta F508/\Delta F508}$ (gut-corrected) mice were intranasally infected with a mix of 10^7 CFUs of all 17 CF *P. aeruginosa* isolates. (**G**) Succinate in BAL (three to eight mice per group pooled from $n = 3$). (**H** to **J**) Neutrophils, monocytes, and alveolar macrophages found in BAL 48 hours after infection (eight mice per group pooled from $n = 3$). (**K** and **L**) *P. aeruginosa* burden in BAL and lungs (eight mice per group pooled from $n = 3$). *Ptenl*$^{-/-}$ mice were intranasally infected with a mix of 10^7 CFUs of all 17 CF *P. aeruginosa* isolates (three to six mice per group pooled from $n = 3$). The following were analyzed: (**M**) succinate in BAL; (**N**) IL-1β in BAL;

(**O** to **Q**) monocytes, neutrophils, and alveolar macrophages found in BAL 24 hours after infection, (**R** and **S**) *P. aeruginosa* burden in BAL and lungs 24 hours after infection. Data are shown as means ± SEM. (A and B) Kaplan-Meier; (C) two-way ANOVA; (D to G and M to S) one-way ANOVA; (H to L) Student's *t* test. *****P* < 0.0001; ****P* < 0.001; ***P* < 0.01; **P* < 0.05.